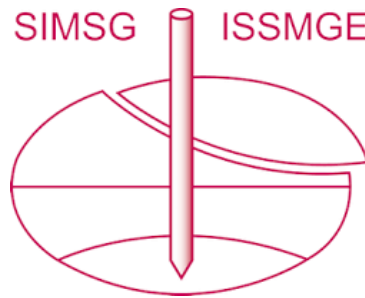


# INTERNATIONAL SOCIETY FOR SOIL MECHANICS AND GEOTECHNICAL ENGINEERING



*This paper was downloaded from the Online Library of the International Society for Soil Mechanics and Geotechnical Engineering (ISSMGE). The library is available here:*

<https://www.issmge.org/publications/online-library>

*This is an open-access database that archives thousands of papers published under the Auspices of the ISSMGE and maintained by the Innovation and Development Committee of ISSMGE.*

*The paper was published in the proceedings of the 20<sup>th</sup> International Conference on Soil Mechanics and Geotechnical Engineering and was edited by Mizanur Rahman and Mark Jaksa. The conference was held from May 1<sup>st</sup> to May 5<sup>th</sup> 2022 in Sydney, Australia.*

# Conceptual framework for determination of volume changes in expansive clays

## Cadre conceptuel pour la détermination du changement de volume dans les argiles expansives

Maki Ito, **Shahid Azam**

Environmental Systems Engineering, University of Regina, Canada  
shahid.azam@uregina.ca

Wayne Clifton

Clifton Associates Limited, Canada

**ABSTRACT:** The main objective of this research was to develop a conceptual framework for the determination of volumetric changes in expansive clays. Based on laboratory investigations and data interpretation, a continuous soil property function (similar to the coefficient of consolidation) was developed. The fundamental concepts of unsaturated soil mechanics (water retention curve, swell-shrink curve, and hydraulic conductivity curve) were used in conjunction with the consolidation curve. The proposed function can be used in the diffusion equation to determine swelling and shrinkage in highly plastic soils.

**RÉSUMÉ :** L'objectif principal de cette recherche était de développer un cadre conceptuel pour la détermination des changements volumétriques dans les argiles expansives. Sur la base des enquêtes de laboratoire et de l'interprétation des données, une fonction continue de propriété du sol (similaire au coefficient de consolidation) a été développée. Les concepts fondamentaux de la mécanique des sols non saturés (courbe de rétention d'eau, courbe de gonflement-rétrécissement et courbe de conductivité hydraulique) en conjonction avec la courbe de consolidation. La fonction proposée peut être utilisée dans l'équation de diffusion pour déterminer le gonflement et le rétrécissement dans les sols à haute plasticité.

**KEYWORDS:** Expansive clays, Volumetric deformations, Soil properties, Conceptual framework

## 1 INTRODUCTION

Expansive clays are susceptible to large volumetric deformations due to changes in soil suction under applied loading (Al-Rawas et al., 2006). Alternate swelling and shrinkage movement near ground surfaces particularly affect civil infrastructure (pipelines, highways) and residential construction (Ito et al., 2014). In North America, estimates indicate that economic losses due to these highly plastic clay problems far exceed the combined cost of all other natural hazards (Huang and Azam, 2020). The general design practice for such soils is to calculate total heave or settlement based on conventional laboratory testing that provides constant indices. As such, movements due to gradual suction changes along with variable hydraulic conductivity and volume compressibility are not well understood.

Terzaghi (1943) used the diffusion equation to develop the consolidation theory based on change in excess pore pressure due to applied stress and assuming constant compressibility and conductivity coefficients. A similar approach was adopted to correlate volume change behavior using soil suction as the primary gradient. Through constant coefficients, Mitchell (1984) developed a method to predict shrinkage and Wray et al. (2005) extended the same to incorporate swelling in clays. However, soil properties become functions of soil suction under saturated-unsaturated conditions (Fredlund et al., 2012). Therefore, there is a need to understand swelling and shrinkage in expansive clays by treating soil properties as continuous functions.

The main objective of this research was to develop a conceptual method for the determination of volumetric changes in expansive clays. Based on laboratory investigations and data interpretation, a continuous soil property function (similar to the coefficient of consolidation) is developed using the water retention curve (WRC), the swell-shrink curve (SSC), the hydraulic conductivity curve (HCC), and the consolidation curve.

## 2 LABORATORY INVESTIGATIONS

The soil was retrieved from a site in Regina (Canada) as per the ASTM Standard Practice for Thin-Walled Tube Sampling of Soils for Geotechnical Purposes (D 1587M-15). The samples were carefully transported to the Advanced Geotechnical Testing Laboratory at the University of Regina and stored at 23°C. These operations followed the ASTM Standard Practice for Preserving and Transporting Soil Samples (D 4220M-14).

Index properties were determined by the following ASTM methods: specific gravity ( $G_s$ ) by the Standard Test Methods for Specific Gravity of Soil Solids by Water Pycnometer (D854-14); grain size distribution (GSD) by the Standard Test Method for Particle-Size Analysis of Soils (D422-63(2007)); and liquid limit ( $w_l$ ), plastic limit ( $w_p$ ) and plasticity index ( $I_p$ ) by the Standard Test Methods for Liquid Limit, Plastic Limit, and Plasticity Index of Soils (D4318-17). Likewise, the shrinkage limit ( $w_s$ ) was estimated using the plasticity chart, as described in Holtz and Kovacs (1981). The samples were classified according to the Standard Practice for Classification of Soils for Engineering Purposes (Unified Soil Classification System) (D2487-17).

The suction values for the WRC were determined following the ASTM Standard Test Methods for Determination of the Soil Water Characteristic Curve for Desorption Using a Hanging Column, Pressure Extractor, Chilled Mirror Hygrometer, and/or Centrifuge (D6836-16). The pressure plate/membrane extractors (Soil Moisture Equipment Inc) were used for up to 1500 kPa suction and the dew point potentiometer (WP4-T, METER Environment) was used for suction values in excess of 1500 kPa. Similarly, the void ratio ( $e$ ) for the SSC was determined in accordance with the ASTM Standard Test Method for Shrinkage Factors of Soils by the Wax Method (D4943-18). In both cases, the gravimetric water content was determined following the Standard Test Methods for Laboratory Determination of Water (Moisture) Content of Soil and Rock by Mass (D2216-19).

Volume changes were obtained as per the ASTM Standard Test Methods for One-Dimensional Swell or Settlement Potential of Cohesive Soils, Method B (D4546- 14). A load frame (Model S-449) along with a 64 mm diameter fixed ring (Model S-455), both manufactured by Durham Geo Slope Indicator Inc., were used. The sample was allowed to undergo swelling under a seating load (half of the field overburden pressure to observe measurable volumetric change). Once the swelling ceased, the soil was incrementally loaded and unloaded to determine the consolidation and rebound properties in accordance with the ASTM Standard Test methods for One-Dimensional Consolidation Properties of Soils Using Incremental Loading (D2435M-11). For each load increment in the consolidation test, the saturated hydraulic conductivity ( $k_s$ ) was calculated using the graphical method developed by Taylor (1948).

## 2 TEST RESULTS

Figure 1 shows grain size distribution curve. Material finer than 0.075 mm measured to be 98% whereas the clay size fraction (material finer than 0.002 mm) was found to be 64%. With a  $G_s$  of 2.76 and high consistency limits ( $w_l = 72\%$ ,  $w_p = 27\%$ ,  $w_s = 14\%$ ), the clay indicated a high water adsorption capacity. The soil was classified as inorganic clays of high plasticity (CH). The measured GSD data were fitted using a pedo-transfer function ( $P_p$ ) according to the following equation (Fredlund et al., 1997):

$$P_p = \frac{1}{\ln[\exp(1) + (\frac{\alpha_1}{d})^{n_1}]^{m_1}} \left\{ 1 - \left[ \frac{\ln(1 + \frac{d_r}{d})}{\ln(1 + \frac{d_r}{d_m})} \right]^7 \right\} \quad (1)$$

where  $\alpha_1$  (0.00307) is related to the initial break point of the curve,  $n_1$  (1.57143) is related to the steepest slope of the curve,  $m_1$  (0.94826) is related to the shape of the fines portion of the curve,  $d_r$  (0.001) is related to the amount of fines in the soil,  $d$  is the diameter of particle size under consideration, and  $d_m$  (0.0001) is the diameter of the minimum allowable particle size.

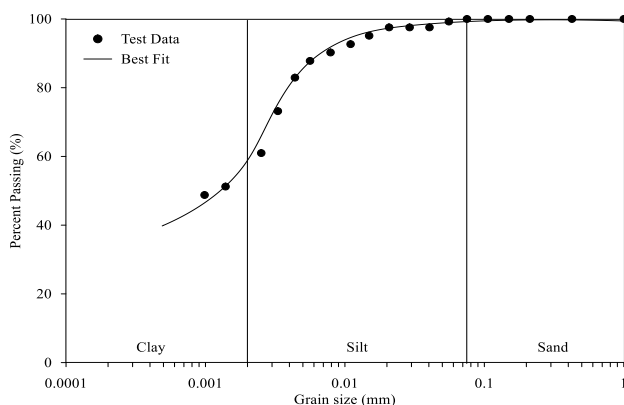


Figure 1. Grain size distribution.

Figure 2 shows the WRC in the form of water content ( $w$ ) versus soil suction ( $\psi$ ). The measured data fitted well with the following equation (van Genuchten, 1980):

$$w = w_r + (w_{sat} - w_r) \left[ \frac{1}{1 + (\alpha_2 \psi^{n_2})} \right]^{m_2} \quad (2)$$

where  $w_r$  (0.05) is the residual gravimetric water content,  $w_{sat}$  (0.41) is the saturated water content,  $\alpha_2$  ( $2 \times 10^{-8}$ ),  $n_2$  (0.25644), and  $m_2$  (9.19744) are fitting parameters. The WRC did not show distinct inflexion points but followed gradual curvature due to over-consolidation (Fredlund, 1964).

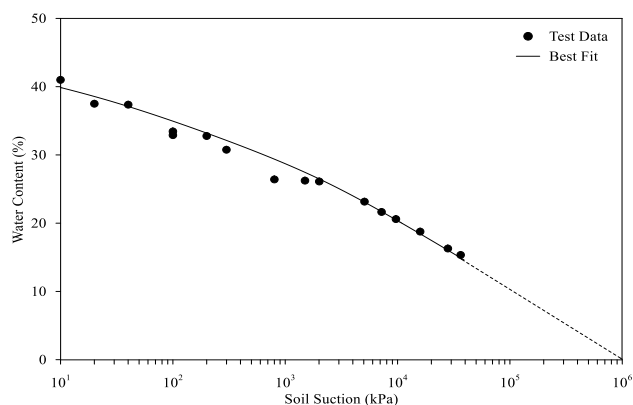


Figure 2. Water retention curve.

Figure 3 presents the SSC in the form of void ratio versus water content with theoretical lines representing various degree of saturation ( $S$ ) values obtained from basic phase relationship. The SSC curve comprises an initial low structural shrinkage followed by a sharp decline during normal shrinkage and then by a low decrease during residual shrinkage (Haines, 1923). This behavior is attributed to fissures in the over-consolidated clay (Ito and Azam, 2020). These hairline cracks developed because of spatio-temporal variations of deformation and stresses arising from cyclic processes of glacial advances and retreats, clay mineral hydration and dehydration, and ice lens formation and disintegration (Ito and Azam, 2013). The measured SSC data fitted well with the following sigmoidal equation:

$$e = \frac{A}{1 + B \exp(-Cw)} + D \quad (3)$$

where  $e$  = void ratio,  $A = 0.6098$ ,  $B = 224.146$ ,  $C = 0.21494$ , and  $D = 0.52948$  are fitting parameters.

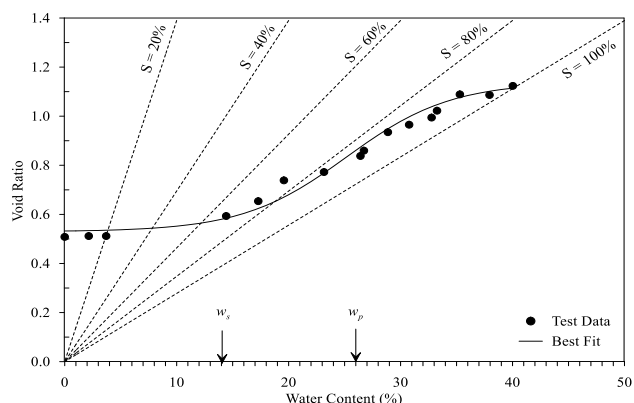


Figure 3. Swell-shrink curve.

Figure 4 shows the HCC. The saturated hydraulic conductivity ( $k_s$ ) measured  $8 \times 10^{-7}$  m/s was used as the initial condition. Likewise, the unsaturated hydraulic conductivity ( $k_\psi$ ) was estimated by using the following equations (Mualem, 1976; van Genuchten 1980):

$$k_\psi = k_s S_e^l \left[ 1 - (1 - S_e)^{\frac{1}{m_2}} \right]^{m_2} \quad (4)$$

$$S_e = (w - w_r) / (w_{sat} - w_r) \quad (5)$$

where  $l$  ( $S$ ) is a fitting parameter and  $S_e$  is a scale factor based on water contents.

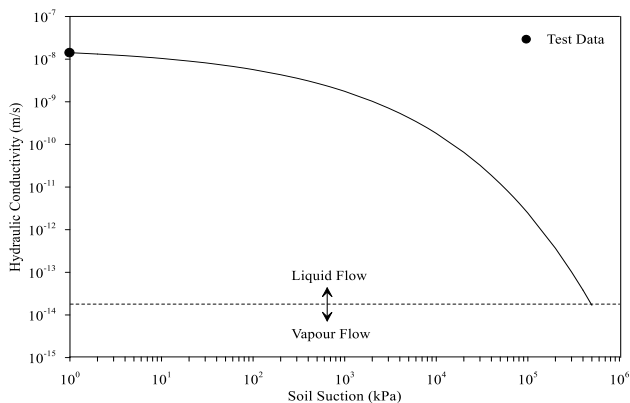


Figure 4. Hydraulic conductivity curve.

The HCC closely matched the shape of the WRC and gradually reduced to  $2 \times 10^{-14}$  m/s where vapor flow became dominant around  $3 \times 10^5$  kPa suction (Ebrahimi-Birang et al., 2004).

Figure 5 gives the change in void ratio in relation to the applied pressure during the free swelling and consolidation tests. The sample increased from the in situ void ratio to a maximum value due to water inundation. Thereafter, the sample was incrementally loaded and unloaded to obtain the compression curve and the rebound curve, respectively. The pre-consolidation pressure ( $\sigma_c$ ) was determined to be 190 kPa representing an over-consolidated clay when compared with the field overburden pressure of 52 kPa. Similarly, the compression index ( $C_c = 0.25$ ) and the swelling index ( $C_s = 0.05$ ) fell within the range typical of inorganic silty clays. Although corresponding to a different site, the current data for the expansive Regina clay closely follow those reported earlier by Azam et al. (2013).

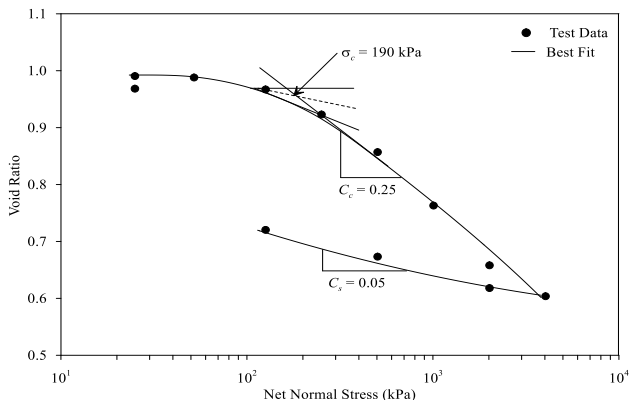


Figure 5. Swell-consolidation-rebound relationship.

### 3 DATA INTERPRETATION

To correlate volume changes with soil suction, the WRC needs to be presented using void ratio on the y-axis. The water content obtained from the  $w$ -based WRC (Eq. 2) was used to determine the corresponding void ratio from the SSC (Eq. 3). This void ratio was compared with that obtained for the corresponding suction from the following equation:

$$e = e_r + (e_{sat} - e_r) \left[ \frac{1}{1 + (\alpha_3 \psi^{n_3})} \right]^{m_3} \quad (6)$$

Computational optimization was carried to estimate Eq. 6 coefficients:  $e_r = 0.539$  (residual void ratio),  $e_{sat} = 1.114$  (saturated void ratio), and fitting parameters, namely;  $\alpha_3 =$

$0.00004$ ,  $n_3 = 0.651$ , and  $m_3 = 3.009$ . To validate Eq. 6, the  $w$ -based WRC was determined by using the fitted GSD (Eq. 1) according to the following equation (Fredlund and Xing, 1994):

$$w = w_s \left[ 1 - \frac{\ln(1 + \frac{w}{h_r})}{\ln(1 + \frac{10^6}{h_r})} \right] \left[ \frac{1}{\left\{ \ln \left[ \exp(1) + \left( \frac{\psi}{\alpha_4} \right)^{n_4} \right] \right\}^{m_4}} \right] \quad (7)$$

where  $h_r$  (0.001) represents soil suction ( $\psi$ ) at residual water content, and fitting parameters of  $\alpha_4$  (0.0004) for inflection point suction,  $n_4$  (0.9355) for desaturation rate, and  $m_4$  (6.5500) for curvature at high suction. These data were converted to obtain the  $e$ -based WRC using the SSC fit (Eq. 6).

Figure 6 presents the WRC in the form of void ratio versus soil suction. Similar to the presentation of Ito and Azam (2013), the two curves derived independently through the GSD data (Figure 1) and the test results corresponded well. Both curves comprised three segments including an initial negligible volume decrease followed by a rapid volume decrease and then by no volume decrease. This means that the void ratio and soil suction relationship can be estimated reasonably well without conducting the WRC and SCC testing.

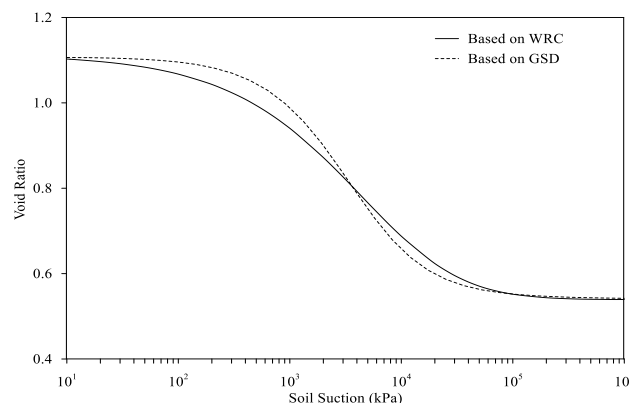


Figure 6. Void ratio versus soil suction relationship.

Figure 7 plots the normalized void ratio versus net normal stress and soil suction. The consolidation curve (Figure 5) and the  $e$ -based WRC (Figure 6) were normalized using the corresponding initial void ratios. The two curves closely matched up to 190 kPa that corresponds to the pre-consolidation pressure as well as to the initiation of desaturation. Thereafter, the two curves followed different slopes such that the consolidation curve was relatively steeper than the WRC. This is because normal stress is more effective than soil suction in reducing the void ratio of the investigated soil (Fredlund et al., 2012).

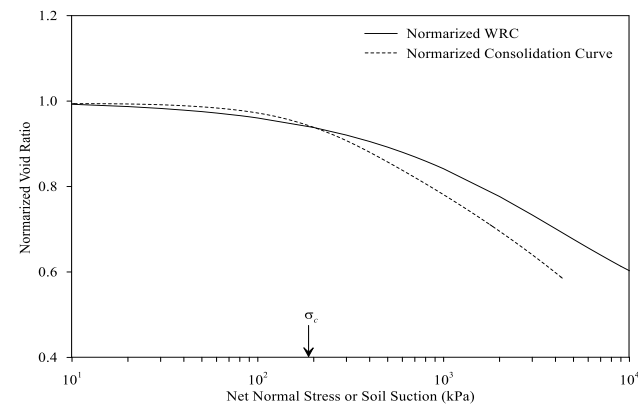


Figure 7. Normalized void ratio versus stress relationships

The coefficient of volume change ( $C_{vc}$ ), similar to the coefficient of consolidation, is given by the following equation:

$$C_{vc} = \frac{k_{\psi} (1+e_0)}{\gamma_w a_{vc}} \quad (8)$$

In the above equation,  $k_{\psi}$  was obtained from Figure 4, initial void ratio ( $e_0$ ) pertained to field conditions, unit weight of water ( $\gamma_w$ ) is constant, and the term  $a_{vc} = de/d\psi$  was obtained from Eq. 6.

Figure 8 gives the soil property function versus soil suction. The  $C_{vc}$  represents a continuous non-linear function and has the units of  $m^2/s$ . For the investigated soil, the shape of the  $C_{vc}$  followed that of the HCC and reduced from  $6.5 \times 10^{-6} m^2/s$  to  $5.1 \times 10^{-12} m^2/s$  over the investigated range of soil suction.

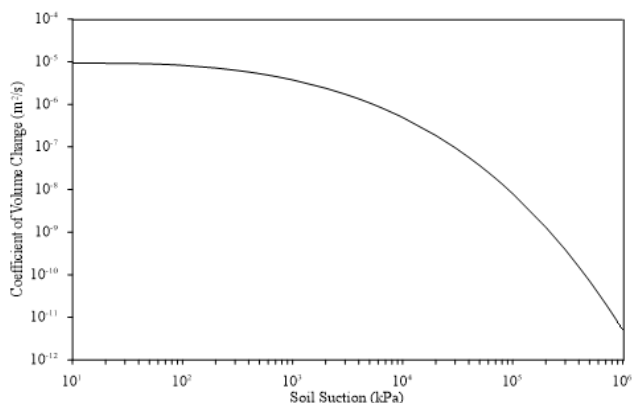


Figure 8. Coefficient of volume change versus soil suction

The soil property function can be determined following a simple procedure based on routine laboratory tests: (i) measure GSD curve and determine the best fit using a pedo-transfer function; (ii) estimate the WRC using the best fit of GSD; (iii) estimate HCC from  $k_s$  and WRC; (iv) measure SSC and determine the best fit using Eq. 2; (v) convert  $w$ -based WRC to  $e$ -based WRC using SSC to determine the derivative ( $a_{vc} = de/d\psi$ ); and (vi) estimate  $C_{vc}$  using Eq. 8.

#### 4 CONCLUSIONS

This research developed a continuous property function using the fundamentals of unsaturated soil mechanics and similar to the coefficient of consolidation. For this purpose, the water retention curve, the swell-shrink curve, the hydraulic conductivity curve, and the consolidation curve were investigated. The proposed function can be used in the diffusion equation to determine swelling and shrinkage. This will help improve design practice for new construction and existing facilities in expansive soils.

#### 5 ACKNOWLEDGEMENTS

The authors would like to acknowledge Clifton Associates Limited and MITACS for providing financial support and the University of Regina for providing laboratory space and computing facilities. Thanks to Mr. Allen Kelly for his assistance in providing soil samples.

#### 6 REFERENCES

Al-Rawas A.A., Goosen M.F.A., and Al-Rawas G.A. 2006. Geology, classification, and distribution of expansive soils and rocks. *Expansive Soils Recent Advances in Characterization and*

*Treatment*. 1:3–14  
 ASTM Standard Practice for Classification of Soils for Engineering Purposes (Unified Soil Classification System). Annual Book of ASTM Standards, West Conshohocken (D2487-17e1).  
 ASTM Standard Practices for Preserving and Transporting Soil Samples (D4220M-14)  
 ASTM Standard Practice for Thin-Walled Tube Sampling of Fine-Grained Soils for Geotechnical Purposes (D1538M-15)  
 ASTM Standard Test Methods for Determination of the Soil Water Characteristics Curve for Desorption Using a Hanging Column, Pressure Extractor, Chilled Mirror Hygrometer, and/or Centrifuge (D 6836-16).  
 ASTM Standard Test Methods for Laboratory Determination of Water (Moisture) Content of Soil and Rock by Mass (D 2216-19).  
 ASTM Standard Test Methods for Liquid Limit, Plastic Limit, and Plasticity Index of Soils (D 4318-17e1).  
 ASTM Standard Test Method for One-Dimensional Consolidation Properties of Soils Using Incremental Loading (D2435-11(2020)).  
 ASTM Standard Test Methods for One-Dimensional Swell or Collapse of Cohesive Soils (D4546-14e1).  
 ASTM Standard Test Method for Particle-Size Analysis of Soils (D 422-63(2007)).  
 ASTM Standard Test Methods for Shrinkage Factors of Soils by the Wax Method (D4943-18).  
 ASTM Standard Test Method for Specific Gravity of Soil Solids by Water Pycnometer (D 854-14).  
 Azam S., Shah I., Raghunandan M.E., and Ito M. 2013. Study on swelling properties of an expansive soil deposit in Saskatchewan, Canada. *Bulletin of Engineering Geology and the Environment*, 72:25-35.  
 Ebrahimi-Birang N., Gitirana Jr G.F.N., Fredlund D.G., Fredlund M.D., and Samarasekera L. 2004. A lower limit for the water permeability coefficient. *Proceedings, 5<sup>th</sup> Canadian Geotechnical Conference*, Quebec, QC, Canada.  
 Fredlund D.G. 1964. Comparison of soil suction and one-dimensional consolidation characteristics of a highly plastic clay. Technical Paper No. 245, National Research Council of Canada Division of Building Research, Ottawa, ON.  
 Fredlund D.G., Rahardjo H., and Fredlund M.D. 2012. *Unsaturated soil mechanics in engineering practise*. John Wiley & Sons, Inc., New York.  
 Fredlund D.G. and Xing A. 1994. Equation for the soil-water characteristics curve. *Canadian Geotechnical Journal*, 31:521-532.  
 Fredlund M.D., Wilson G.W., and Fredlund D.G. 1997. Prediction of the soil-water characteristics curve from the grain size distribution curve. *Proceedings, 3<sup>rd</sup> Symposium on Unsaturated Soil*, Rio de Janeiro, Brazil, 12-23.  
 Haines W.B. 1923. The volume change associated with variations of water content in soil. *Journal of Agricultural Science*, 13:296–310.  
 Holtz W.G. and Kovacs W.D. 1981. *An Introduction to Geotechnical Engineering*. Prentice-Hall Inc., Englewood Cliffs, NJ, USA.  
 Huang Q. and Azam S. 2020. Evaluation of empirically predicted volumetric changes in cracked expansive clays. *Innovative Infrastructure Solutions*, 5:104.  
 Ito M. and Azam S. 2020. Relation between flow through and volumetric changes in natural expansive soils. *Engineering Geology*, 279:105885.  
 Ito M. and Azam S. 2013. Engineering properties of a vertisolic expansive soil deposit. *Engineering Geology*, 152:10–16  
 Ito M., Azam S., and Hu Y (2014). A two stage model for moisture-induced deformations in expansive soils. *Environmental Systems Research*. 3(19):1-11.  
 Mitchell P.W. 1984. A simple method of design of shallow footings on expansive soil. *Proceedings, 5<sup>th</sup> International Conference on Expansive Soils*, Adelaide, South Australia, 1-8.  
 Mualem Y. 1976. A new model for predicting the hydraulic conductivity of unsaturated porous media. *Water Resource Research*, 12:513-522.  
 Taylor D.W. 1948. *Fundamentals of Soil Mechanics*. Wiley, New York, NY, USA.  
 van Genuchten, M.Th. 1980. A Closed-form Equation for Predicting the Hydraulic Conductivity of Unsaturated Soils1. *Soil Science Society of America Journal*, 44:892-898.  
 Wray W.K., El-Garhy B.M., and Youssef A.A. 2005. Three-dimensional model for moisture and volume change prediction in expansive soils. *Journal of Geotechnical and Geoenvironmental Engineering*, 131:311-324.